Electronic Supplementary Material (ESI) for Materials Advances.

Supplementary Information

Electrochemically Exfoliated Graphene/poly(3,4-ethylenedioxythiophene) Nanocomposite based Electrochemical Sensor for Detection of Nicotine

Jerome Rajendran[1], Anatoly N. Reshetilov[2] and Ashok K. Sundramoorthy[1,*]

[1]Department of Chemistry, SRM Institute of Science and Technology, Kattankulathur-603 203, Tamil Nadu, India

[2]G.K. Skryabin Institute of Biochemistry and Physiology of Microorganisms of the Russian Academy of Sciences (IBPM RAS), Subdivision of "Federal Research Center Pushchino Biological Research Center of the Russian Academy of Sciences" (FRC PBRC RAS), 142290, Pushchino142290, Moscow oblast, Russia

***Corresponding author**

Email: ashokkus@srmist.edu.in

Scheme

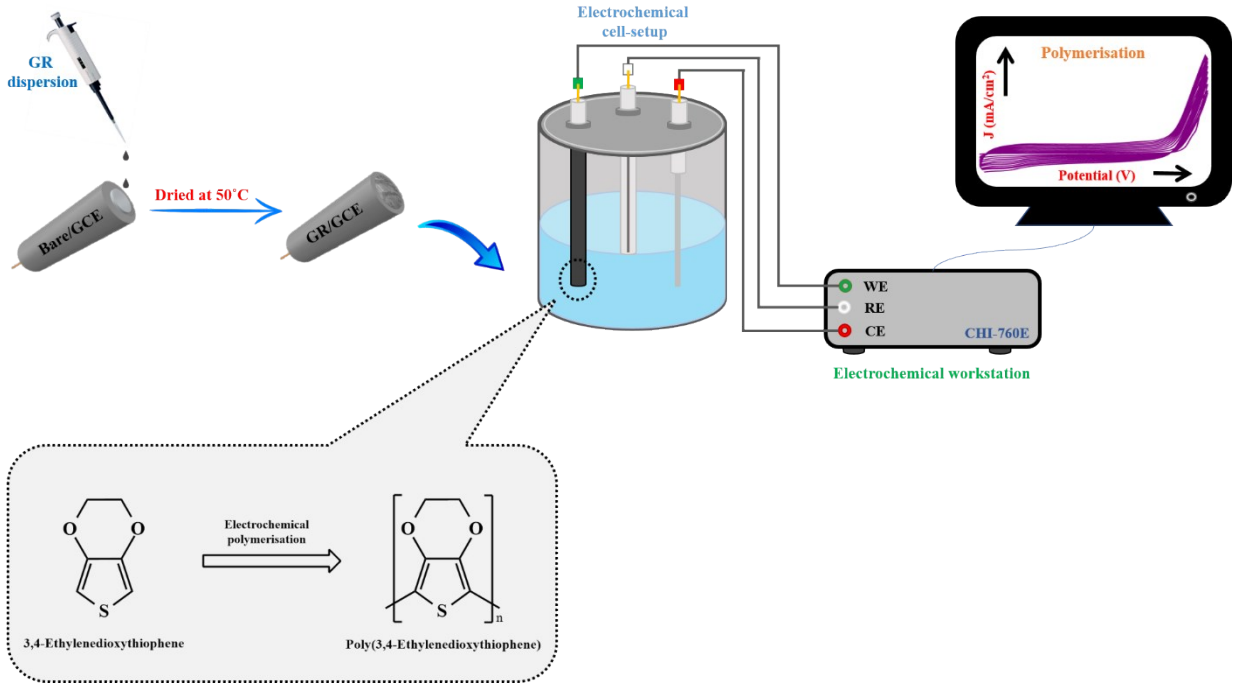

Scheme S1. (a) Preparation of PEDOT/GR/GCE and (b) polymerization of EDOT on the GR/GCE surface.

Supplementary Figures

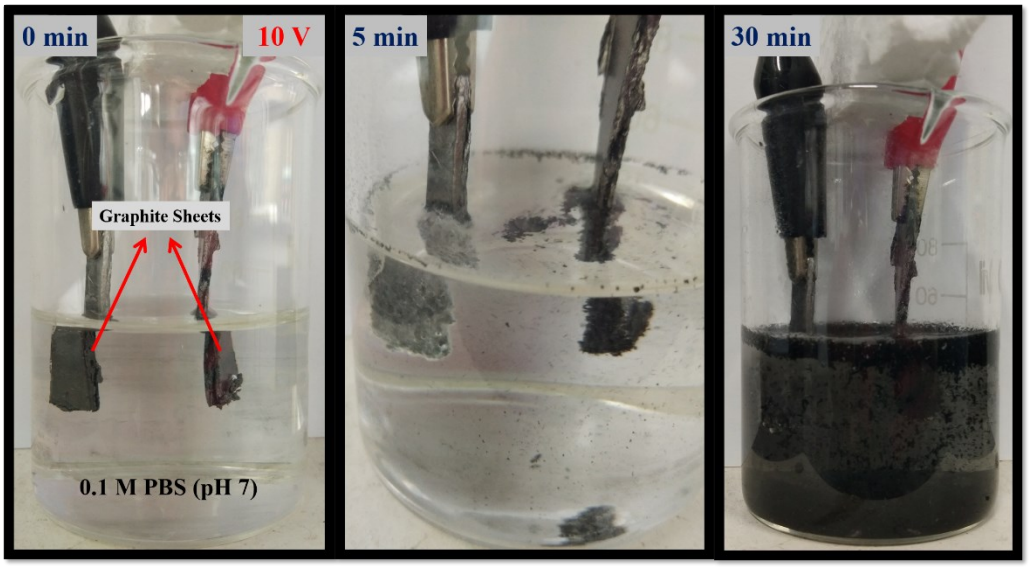

Fig. S1 Photographic images of GR synthesized by electrochemical exfoliation method using graphite sheet electrodes in PBS. (The images shows the exfoliation of GR nanosheets during the electro-chemical process at 10 V for 0 to 30 min).

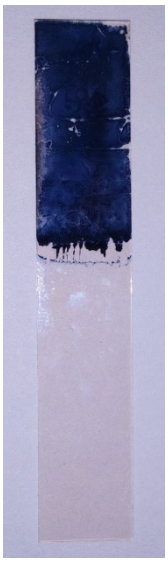

Fig. S2 Photographic images of electrochemically polymerized PEDOT on ITO (Indium tin oxide electrode). (To reveal the polymer color, the polymerization was carried on the transparent ITO electrode and the image clearly indicated that polymer color was dark blue on the electrode surface).

Fig. S3 Photographic image of (a) ten different brand cigarettes and (b) after the removal of filters, rolling papers and (c) obtained tobacco powder from the cigarettes.

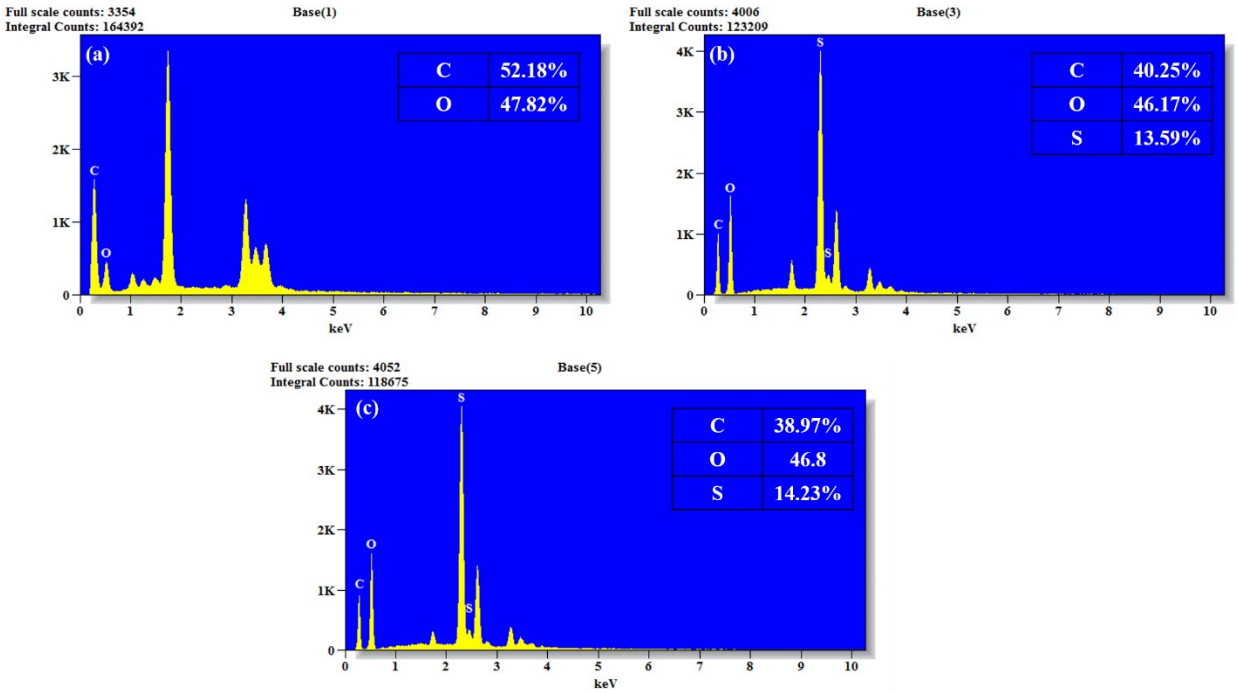

Fig. S4 EDX spectra of (a) GR, (b) PEDOT and (c) PEDOT/GR (inset table: atomic percentages of the elements).

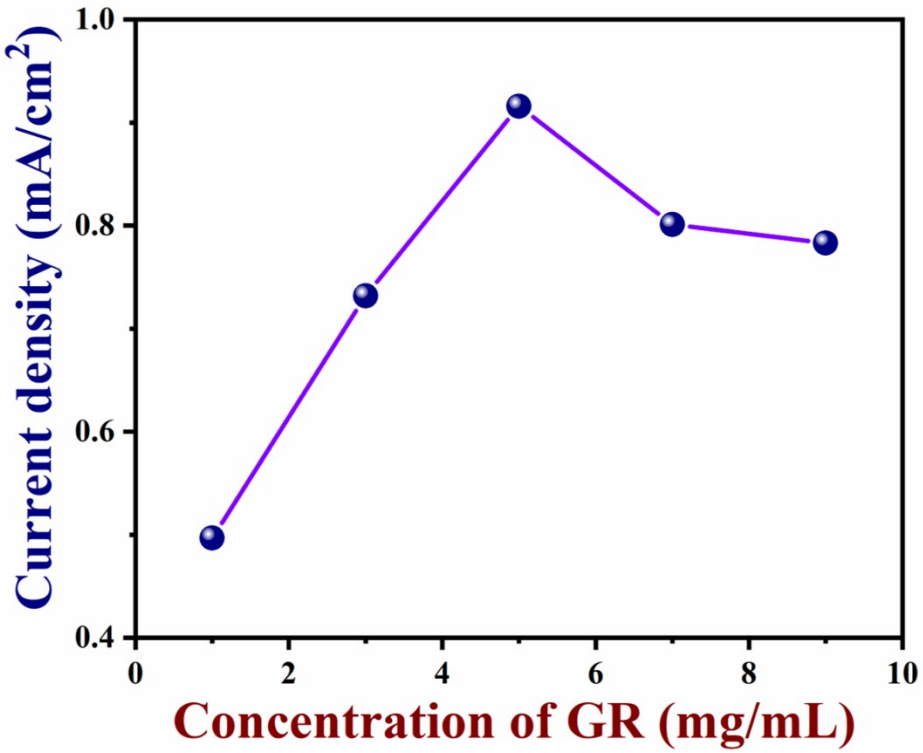

Fig. S5 Plot of different modified electrodes vs. ΔE_p and R_{ct} values.

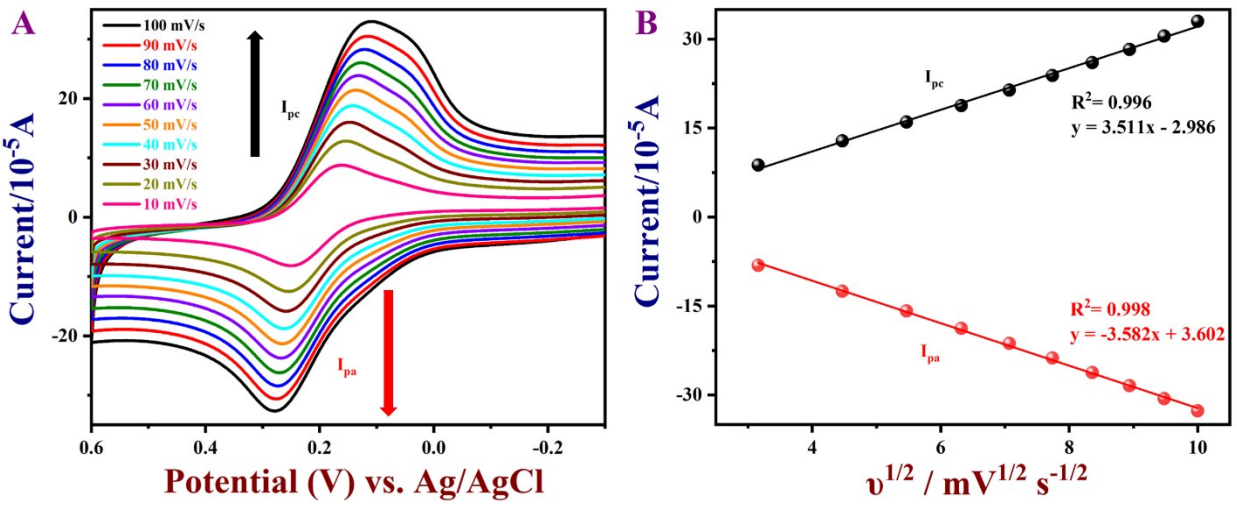

Fig. S6 (A) Different scan rates of PEDOT/GR/GCE in 0.1 M KCl containing 5 mM $[Fe(CN)_6]^{3-/4-}$ and (B) The linear plots of redox peak currents vs. $\upsilon^{1/2}$.

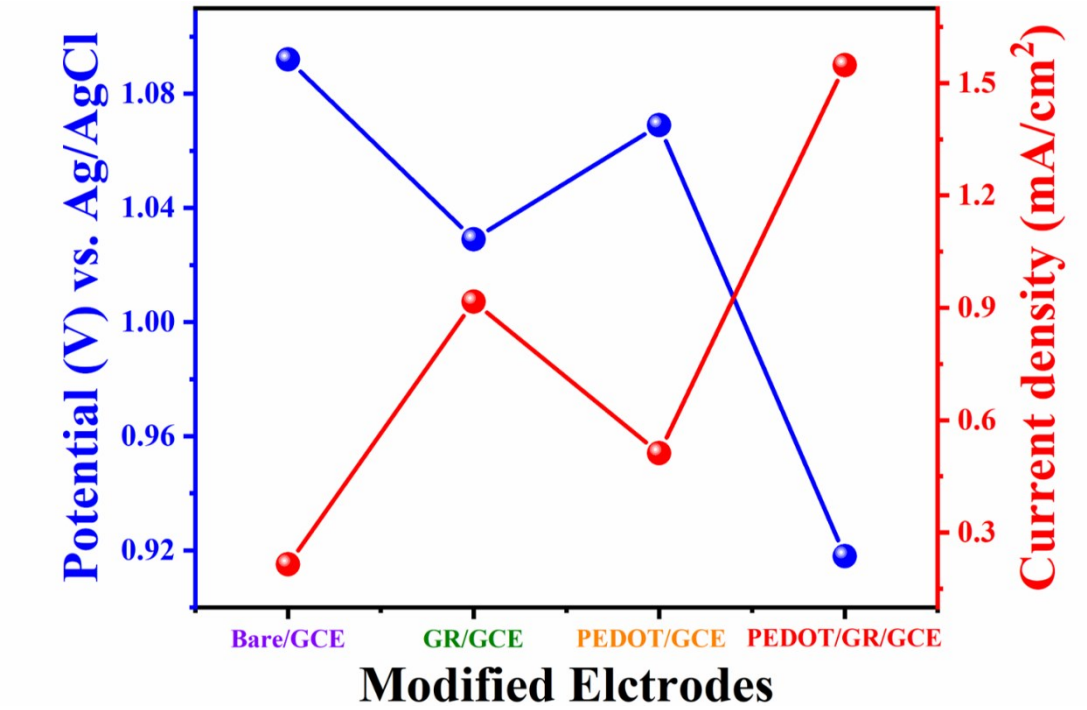

Fig. S7 Plot of various modified electrodes vs. nicotine oxidation potential and current density.

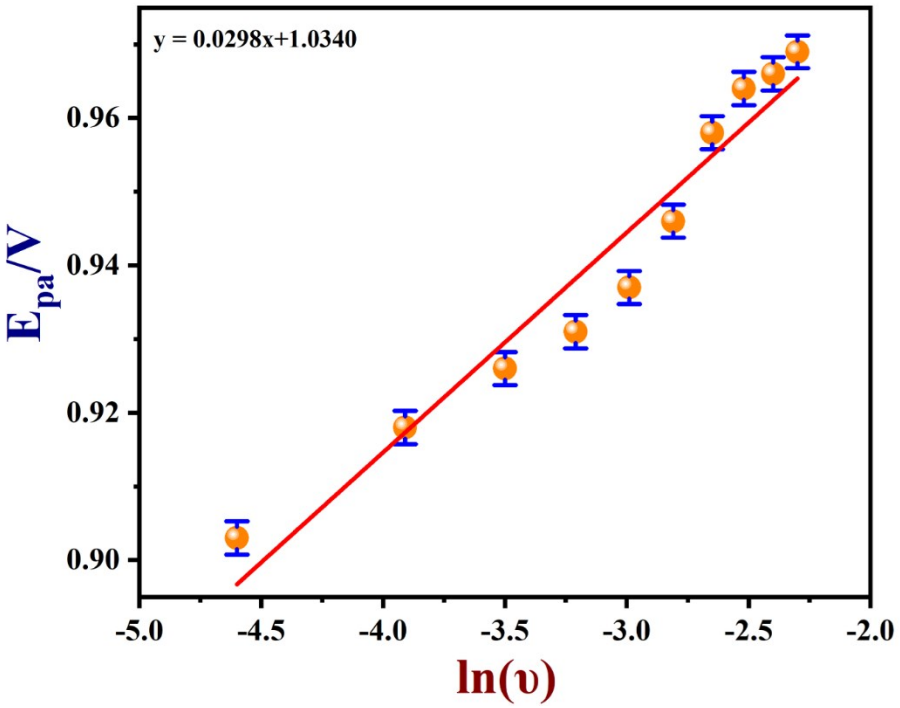

Fig. S8 The plot of oxidation peak potential (E_{pa}) vs. the natural logarithm of scan rate (ln υ).

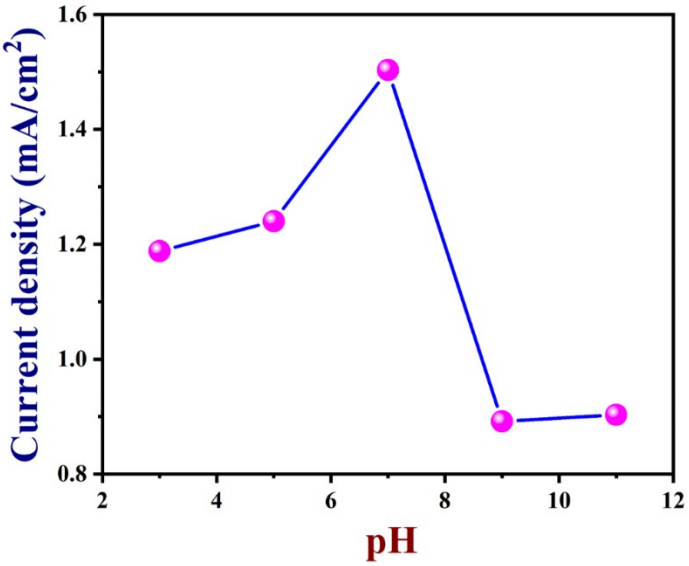

Fig. S9 The plot of nicotine oxidation peak current density vs. pH

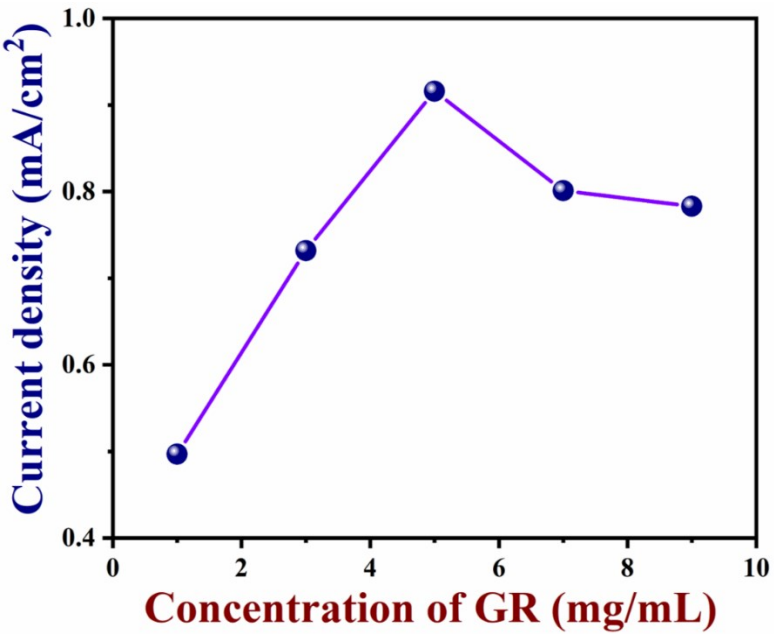

Fig. S10 The effects of catalyst loading (1 to 9 mg/mL) on the oxidation of nicotine. A relationship between the oxidation peak peak currents of nicotine and the amount of GR loaded on GCE.

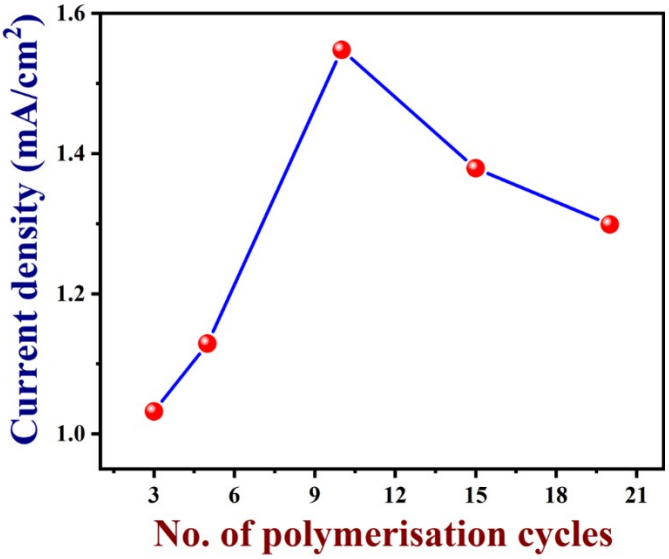

Fig. S11 The plot of the number of PEDOT polymerization cycles vs. nicotine oxidation currents.

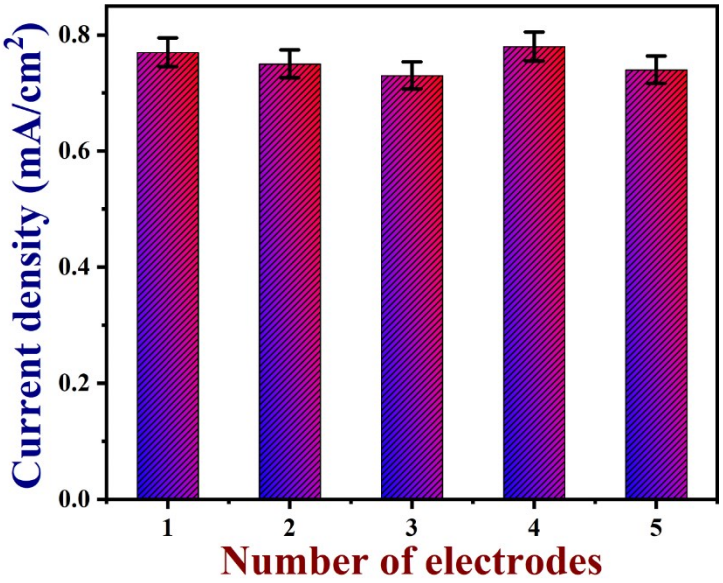

Fig. S12 Histrogram of CV responses recorded for five different PEDOT/GR modified electrodes for the fixed concentration of nicotine (50 μM) oxidation in PBS.

Tables

Table S1. Comparison of analytical parameters of the PEDOT/GR/GCE based electrochemical nicotine sensor with the previously reported sensors.

Electrode	Electrolyte solution	LOD (µM)	Linear range (µM)	Ref.
MWCNT/BPPG electrode	BRBS (pH 8)	1.5	19.2 – 1000	[1]
PEDOT/TiO_2/ITO	PBS (pH 7.4)	4.9	0–5000	[2]
MWCNT/ACS/GCE	PBS (pH 8)	1.42	5-200	[3]
CPE	PBS (pH 7.5)	6.1	50–500	[4]
	BRBS (pH 11)	3.2	50–1000	
PGE	PBS (pH 7) + 2 mM SDS	2	7.6–107.5	[5]
BDDE	BRBS (pH 8)	0.3	0.5–200	[6]
p-AHNSA/GCE	PBS (pH 7.5)	0.8	1-200	[7]
NGS/SPCE	PBS (pH 7.4)	0.04	0-200	[8]
EA/GCE	PBS (pH 7)	0.7	1–200	[9]

DPA/rGO/PGE	$Na_2C_2O_4$ (pH 4.5)	7.6	31–1900	[10]
CNC/SPCE	PBS (pH 7.4)	2	10–1000	[11]
$CuWO_4$/rGO/Nf/GCE	PBS (pH 7)	0.04	0.1–0.9	[12]
BN/graphene/GCE	PBS (pH 7)	0.4	1-1000	[13]
PEDOT/GR/GCE	PBS (pH 7)	0.04	0.5-1000	This Work

(**MWCNT/BPPG electrode** – multi-walled carbon nanotube modified basal plane pyrolytic graphite electrodes; **PEDOT/TiO_2/ITO** – titanium dioxide/PEDOT modified indium tin oxide electrode; **MWCNT/ACS/GCE** – MWCNT and alumina-coated silica nanocomposite modified GCE; **CPE** – carbon paste electrode; **PGE** – pencil graphite electrode; **BDDE** – boron doped diamond electrode; **p-AHNSA/GCE** – poly(4-amino-3-hydroxynaphthalene sulfonic acid) modified GCE; **NGS/SPCE** – nitrogen-doped graphene sheets modified screen printed carbon electrode; **EA/GCE** – electrochemically activated glassy carbon electrode; **DPA/rGO/PGE** – azo dye (E)-1-(4-((4-(phenylamino)phenyl)diazenyl) phenyl) ethanone combined with reduced graphene oxide (rGO) modified pencil graphite electrode; **CNC/SPCE** – carbon nanotube cluster modified screen printed electrodes; **$CuWO_4$/rGO/Nf/GCE** – copper tungstate decorated rGO nanocomposite and nafion immobilized GCE).

Supporting references

1 M. J. Sims, N. V Rees, E. J. F. Dickinson and R. G. Compton, *Sensors Actuators B Chem.*, 2010, **144**, 153–158.

2 C.-T. Wu, P.-Y. Chen, J.-G. Chen, V. Suryanarayanan and K.-C. Ho, *Anal. Chim. Acta*, 2009, **633**, 119–126.

3 S.-J. Wang, H.-W. Liaw and Y.-C. Tsai, *Electrochem. commun.*, 2009, **11**, 733–735.

4 M. Stočes and I. Švancara, *Electroanalysis*, 2014, **26**, 2655–2663.

5 A. Levent, Y. Yardim and Z. Senturk, *Electrochim. Acta*, 2009, **55**, 190–195.

6 Ľ. Švorc, D. M. Stanković and K. Kalcher, *Diam. Relat. Mater.*, 2014, **42**, 1–7.

7 A. Geto, M. Amare, M. Tessema and S. Admassie, *Electroanalysis*, 2012, **24**, 659–665.

8 X. Li, H. Zhao, L. Shi, X. Zhu, M. Lan, Q. Zhang and Z. H. Fan, *J. Electroanal. Chem.*, 2017, **784**, 77–84.

9 H. Kassa, A. Geto and S. Admassie, *Bull. Chem. Soc. Ethiop.*, 2013, **27**, 321–328.

10 Y. Jing, B. Yu, P. Li, B. Xiong, Y. Cheng, Y. Li, C. Li, X. Xiao, M. Chen and L. Chen, *Sci. Rep.*, 2017, **7**, 14332.

11 L. Highton, R. O. Kadara, N. Jenkinson, B. Logan Riehl and C. E. Banks, *Electroanalysis*, 2009, **21**, 2387–2389.

12 A. Karthika, P. Karuppasamy, S. Selvarajan, A. Suganthi and M. Rajarajan, *Ultrason. Sonochem.*, 2019, **55**, 196–206.

13 R. Jerome and A. K. Sundramoorthy, *Anal. Chim. Acta*, 2020, **1132**, 110–120.